Biosensors and Bioelectronics 107 (2018) 34–39

Contents lists available at ScienceDirect

Biosensors and Bioelectronics

journal homepage: www.elsevier.com/locate/bios

Signal-on electrochemiluminescence biosensor for microRNA-319a detection based on two-stage isothermal strand-displacement polymerase reaction

Minghui Wang, Yunlei Zhou, Huanshun Yin*, Wenjing Jiang, Haiyan Wang, Shiyun Ai

College of Chemistry and Material Science, Shandong Agricultural University, Taian 271018, PR China

ARTICLE INFO

Keywords:
Isothermal strand-displacement polymerase reaction
Chemical mutagen
Ethyl methanesulfonate
Rice seedlings
Nicking enzyme
DNA polymerase

ABSTRACT

MicroRNAs play crucial role in regulating gene expression in organism, thus it is very necessary to exploit an efficient method for the sensitive and specific detection of microRNA. Herein, a signal-on electrochemiluminescence biosensor was fabricated for microRNA-319a detection based on two-stage isothermal strand-displacement polymerase reaction (ISDPR). In the presence of target microRNA, amounts of trigger DNA could be generated by the first ISDPR. Then, the trigger DNA and the primer hybridized simultaneously with the hairpin probe to open the stem of the probe, and then the ECL signal will be emitted. In the presence of phi29 DNA polymerase and dNTPs, the trigger DNA could be displaced to initiate a new cycle which was the second ISDPR. Due to the two-stage amplification, this method presented excellent detection sensitivity with a low detection limit of 0.14 fM. Moreover, the applicability of the developed method was demonstrated by detecting the change of microRNA-319a content in the leaves of rice seedlings after the rice seeds were incubated with chemical mutagen of ethyl methanesulfonate.

1. Introduction

MicroRNAs are a sort of small noncoding and endogenous RNAs with the length of about 22 nucleotides, which exist in animals, plants and viruses, and play crucial role in gene regulation, cell development, differentiation and apoptosis (Rigoutsos and Furnari, 2010; Winter et al., 2009). Due to the small dimension, low content, and high sequence similarity, there is a certain challenge to its quantitative detection of microRNAs. Therefore, it is essential to develop sensitive, dependable and handy analytical method for microRNA detection (Wang et al., 2014). Up to now, various methods have been developed for microRNA detection, such as electrochemistry (Liu et al., 2017a), photoelectrochemistry (Yin et al., 2016), electrochemiluminescence (ECL) (Chen et al., 2016) and fluorescence (Yin et al., 2017). Compared with other methods, ECL has attracted particular attentions due to its fast response speed, high sensitivity and easy operation (Cui et al., 2017; Feng et al., 2016), which provided a new chance for bioanalysis applications.

ECL material is one of the major parameters for ECL biosensor, which will greatly influence its detection performance. The ECL properties of Ru complex have caused great concern due to their high ECL efficiency, good biocompatibility and stability. Typically, tripropylamine (TPrA) is usually used as co-reagent which could significantly improve the ECL signal intensity of Ru complex, and the ECL signal intensity is proportional to the Ru complex concentration in the case of excess TPrA (Zhou et al., 2014). It suggests that the Ru complex/TPrA system could be applied to the quantitative bioanalysis. Significantly, it has been reported that the ECL signal of Ru complex/TPrA system could be effectively quenched by graphene oxide (GO) due to the poor conductivity and its oxidative functional groups. In addition, GO is an efficient carrier due to its excellent mechanical strength and lager specific surface area (Liu et al., 2017b). For example, Huang et al. developed an ECL sensor for ultrasensitive nucleic acid detection where GO was acted as quencher and exhibited excellent performance (Huang et al., 2015) (More details were shown in Supplementary material). Nevertheless, this method is not sensitive enough for miRNAs detection as miRNAs are trace in cells. This problem can be solved by amplifying the detection signal. When combined with appropriate signal amplification strategy, this method can be applied for the ultrasensitive detection of miRNA.

Various signal amplification strategies, especially DNA isothermal amplification technologies, have been widely applied in the field of biosensors for improve the detection sensitivity, including hybridization chain reaction (HCR) (Schwarzkopf and Pierce, 2016; Xie et al.,

* Corresponding author.
E-mail address: yinhs@sdau.edu.cn (H. Yin).

https://doi.org/10.1016/j.bios.2018.02.015
Received 23 December 2017; Accepted 4 February 2018
Available online 05 February 2018
0956-5663/

2016), rolling circle amplification (RCA) (Goo and Kim, 2016; Kim et al., 2017), isothermal strand-displacement polymerase reaction (ISDPR) (Wang et al., 2017; Zhang et al., 2017), etc. Among these signal amplification strategies, ISDPR attracted great attention since it does not require specific recognition sites, specially designed circular templates and repeated thermal cycling (Wang et al., 2015). In ISDPR, the hybridization between the template and target can induce polymerization reaction which could produce amounts of trigger DNA to replace the target strand. The released target strand combines with another template to initiate next polymerization reaction, resulting in the recovery of the target DNA and the amplification of the signal.

In traditional ISDPR, the thermodynamic properties of the template and primer are unstable which would affect the efficiency of the reaction. To solve this problem, many studies have been carried out by using the coaxial stacking hybridization to improve the stability in recent years. Coaxial stacking hybridization means that two or more paratactic terminal nucleotides hybridized with a longer complementary strand and form a compact head-to-tail structure which would obtain the excellent stability (Arata et al., 2012). Liu et al. (2016) investigated the effect of invading stacking primers (IS-Primer) on the ISDPR efficiency, and found that the IS-Primer could enhance the specificity and sensitivity of the ISDPR (More details were shown in Supplementary material). In the presence of primer, not only the thermodynamic stability of the nucleic acid hybridization was increased, but also the untying efficiency of the hairpin probe was improved.

In this work, we fabricated a signal-on ECL biosensor based on two-stage isothermal strand-displacement polymerase reaction for microRNA-319a detection. The signal was amplified twice by ISDPR. Firstly, target microRNA hybridized with template DNA, and induced polymerization reaction which produced amounts of trigger DNA for the following amplification reaction. This is the first isothermal strand-displacement polymerase reaction. Then, the trigger DNA along with the primer hybridized with the hairpin probe to open the stem of the probe, and then the ECL signal will be emitted. Simultaneously, in the presence of phi29 DNA polymerase and dNTPs, the trigger DNA would be displaced to initiate a new cycle, and this is the second isothermal strand-displacement polymerase reaction. Due to the two-stage amplification, this ECL biosensor exhibited an ultrasensitive detection performance for the target microRNA.

2. Experimental section

2.1. Materials and reagents

See Supplementary material.

2.2. Synthesis of Ru-hp-DNA complex

Ru-hp-DNA complex was prepared according to previous report (Huang et al., 2015). 4.0 mg bis(isothiocyanato)bis(2,2′-bipyridyl-4,4′-dicarboxylato)ruthenium(II) was dispersed in 1 mL of 0.1 M PBS (pH 7.4), and then 100 μL of the Ru complex dispersion was activated by 100 μL of 0.1 M PBS containing NHS (0.5 mg/mL) and EDC (0.5 mg/mL) for 4 h. After that, the Ru complex dispersion was added to the hairpin probe solution, and then shocked at 25 °C for 2 h in a dark place to immobilize the Ru complex on the hairpin probe. After that, 100 μL of 3 M sodium acetate solution and 2 mL of ice anhydrous ethanol were added to the reaction system and standed at 4 °C for 12 h. Subsequently, the obtained mixture was centrifuged with 12,000 rpm for 30 min and the precipitates were collected and washed with 70% of the ice anhydrous ethanol for three times. After dried in vacuum freeze dryer, the precipitates (Ru complex modified hairpin probe) were dispersed in 100 μL of 0.1 M PBS (pH 7.4).

2.3. Preparation of AuNPs/GO/GCE

Glassy carbon electrode (GCE) was firstly polished to mirror-like surface using 0.3 μm alumina slurry, and then sonicated with double-distilled deionized water and anhydrous alcohol for 3 min, respectively. After dried under N_2 blowing, 10 μL of 2 mg/mL graphene oxide dispersion was dripped on the bare GCE surface and dried under the irradiation of infrared lamp. Finally, 10 μL gold nanoparticles (AuNPs) were dripped on electrode surface and dried under irradiation of infrared lamp, where AuNPs were synthesized according to previous report (Liu and Lu, 2006). The obtained electrode was noted as AuNPs/GO/GCE.

2.4. Probe immobilization

Prior to immobilization, 100 μL of 10 μM hairpin probe was mixed with 1 μL of 100 mM TCEP, and incubated for 1 h at room temperature (Qian et al., 2015). Then, the mixed solution was annealed by incubating at 95 °C for five min and cooled down to room temperature naturally to form the hairpin structure.

Afterwards, the 10 μL of the Ru-hp-DNA solution and probe immobilization buffer was mixed, and then it was dropped on AuNPs/GO/GCE surface and incubated for 12 h in a moist environment at 37 °C. The obtained electrode was then washed with washing buffer to remove the unconjugated probe, and it was noted as hp-DNA/AuNPs/GO/GCE. Then, 10 μL of 0.1 M PBS containing 1.0 mM MPA was dropped on the hp-DNA/AuNPs/GO/GCE surface and incubated for 1 h to block the electrode, followed by rinsing with washing buffer.

2.5. Isothermal strand-displacement polymerase reaction

20 μL of 1 μM template DNA, 20 μL of different concentrations of microRNA-319a and 10 μL of 5 × microRNA hybridization buffer were first mixed. Then, the mixed solution was heated to 95 °C for five min and cooled down to room temperature naturally and incubated for 2 h to make the complete hybridization of DNA and microRNA.

After the addition of a 50 μL solution consisting 250 μM dNTPs, 100 U/mL Nt.*Bsm*AI, 100 U/mL phi29 DNA polymerase and 1 × reaction buffer (50 mM Tris-HCL, 10 mM $MgCl_2$, 10 mM $(NH_4)_2SO_4$, 4 mM DTT, 200 μg/mL BSA, 50 mM KCl. pH 7.5), the mixture was incubated for 2.5 h at 37 °C to generate trigger DNA. Then, the reaction was terminated with incubation at 65 °C for 10 min.

2.6. Fabrication of the ECL biosensor

10 μL of DNA hybridization buffer containing products of ISDPR and primer (10 μM) was dropped onto the surface of hp-DNA/AuNPs/GO/GCE and incubated for 2 h at 37 °C. Then, the electrode was rinsed with washing buffer and noted as dsDNA/AuNPs/GO/GCE. Subsequently, the electrode was incubated with 10 μL of polymerase reaction mixture including 100 U/mL phi29 DNA polymerase, 250 μM dNTPs and 1 × phi29 reaction buffer (50 mM Tris-HCL, 10 mM $MgCl_2$, 10 mM $(NH_4)_2SO_4$, 4 mM DTT, 200 μg/mL BSA, pH 7.5) for 2.5 h at 37 °C, and then rinsed with washing buffer.

2.7. ECL detection

The ECL detection was performed at a computerized MPI-A electrochemiluminescence analyzer (Xi'An Remax Electronic Science Technology. Co. Ltd. Xi'An, China) with a photomultiplier tube voltage of 900 V. A conventional three-electrode system was used in the experiment, with a modified GCE as the working electrode, a platinum wire as counter electrode, and Ag/AgCl (saturated KCl) as the reference electrode. ECL measurements were carried out under scanning from 0.2 V to 1.25 V at a scanning rate of 100 mV/s in ECL detection buffer.

2.8. Sample preparation

Mature seeds of rice used in this work were supplied by College of Life Science, Beijing Normal University. These rice seeds were divided into two groups with one group as control sample and the other as detection sample. The detection sample was immersed in aqueous solutions of ethyl methanesulfonate at a concentration of 0.7% for six hours. The control sample was immersed in distilled deionized water for same time. Then, these seeds were washed in running water for four hours. Afterwards, these seeds were embedded in gauze within petri dishes and cultured with double-distilled ionized water for a few days at room temperature for germination. Finally, the leaves of rice seedling were harvested for RNA extraction by using TRIzol® Plus RNA Purification Kit according to the manufacturer' instructions. The concentration of the extracted RNA was determined by UV–vis spectrophotometry. For microRNA detection, the extracted RNA was diluted to the same concentration.

3. Results and discussion

3.1. Detection strategy of the ECL biosensor

In this work, a signal-on electrochemiluminescence biosensor was developed for microRNA-319a detection based on two-stage isothermal strand-displacement polymerase reaction. The detection strategy was illustrated in Scheme 1. Firstly, microRNA-319a hybridized with template DNA, and then the target microRNA-319a can be extended from its 3′ terminal to the 5′ terminal of the template DNA to form a double-stranded DNA in the presence of phi29 DNA polymerase and dNTPs. Meanwhile, the recognition site for the Nt.*Bsm*AI nicking endonuclease is produced, which induces Nt.*Bsm*AI to cut a gap at the extended strand of the double-stranded DNA. Afterwards, the 3′ terminal of microRNA-319a can be extended again and the downstream DNA strand (named as trigger DNA) can be displaced and released. As a result, amounts of trigger DNA can be fabricated and may participate in the following reaction. This is the first isothermal strand-displacement polymerase reaction.

In the next reaction, we used a hairpin probe which labeled with 5′-SH and 3′-NH_2. The bis(isothiocyanato)bis(2,2′-bipyridyl-4,4′-dicarboxylato)ruthenium(II) was immobilized on the hairpin probe through the combination of amino and carboxyl. Then the Ru complex modified hairpin probe was self-assembled on the surface of AuNPs/GO/GCE by the Au-S binding. Herein, we used the Ru complex/TPrA system to provide ECL signal. Due to the oxygenated functional groups and poor conductivity of GO, the ECL signal of Ru complex/TPrA system could be effectively quenched. The stem of the hairpin probe was 11 base pairs and the loop was 20 unpaired nucleotides. The trigger DNA and the loop of the hairpin probe were completely complementary pairing, which made a fraction of the probe stem untied. Simultaneously, the primer hybridized with the untied stem as a close neighbor of the trigger DNA to speed up the untying process of the stem. Afterwards, in the presence of phi29 DNA polymerase and dNTPs, the trigger DNA would be displaced to initiate a new cycle, and this is the second isothermal strand-displacement polymerase reaction. Without the trigger DNA and primer, the hairpin probe was in the folded construction and its termini were close to the GO modified electrode, leading the quenching of the ECL signal. While in the presence of the trigger DNA and primer, the stem of the hairpin probe will be opened, which causes the Ru complex away from the electrode surface, and the biosensor will be in a "signal on" mode.

3.2. Characterization of materials

The morphology of GO and AuNPs were characterized by TEM. Fig. 1A shows the TEM image of GO, which demonstrates that the typical wrinkle structure of GO sheets. Fig. 1B presents the TEM image for AuNPs with the acceptable diameter. Fig. 1C shows the UV–vis absorption spectra of Ru complex (curve a), hairpin probe (curve b) and Ru complex modified hairpin probe (curve c). The absorption spectrum of the Ru complex (curve a) presents a characteristic peak at 502 nm, assigned to the charge transfer from metal to ligand and that at 308 nm, belonged to the charge transfer of $\pi \rightarrow \pi^*$ transitions from ligand to ligand. The remarkable absorption peak of hairpin probe appears at 260 nm (curve b). After modified hairpin probe with Ru complex, the absorption spectrum (curve c) displays both the hairpin probe and the Ru complex remarkable absorption peaks. The typical absorption peak appears at 502 nm, consistenting with the remarkable peak of Ru complex. The characteristic absorption peaks at 248 nm and 306 nm

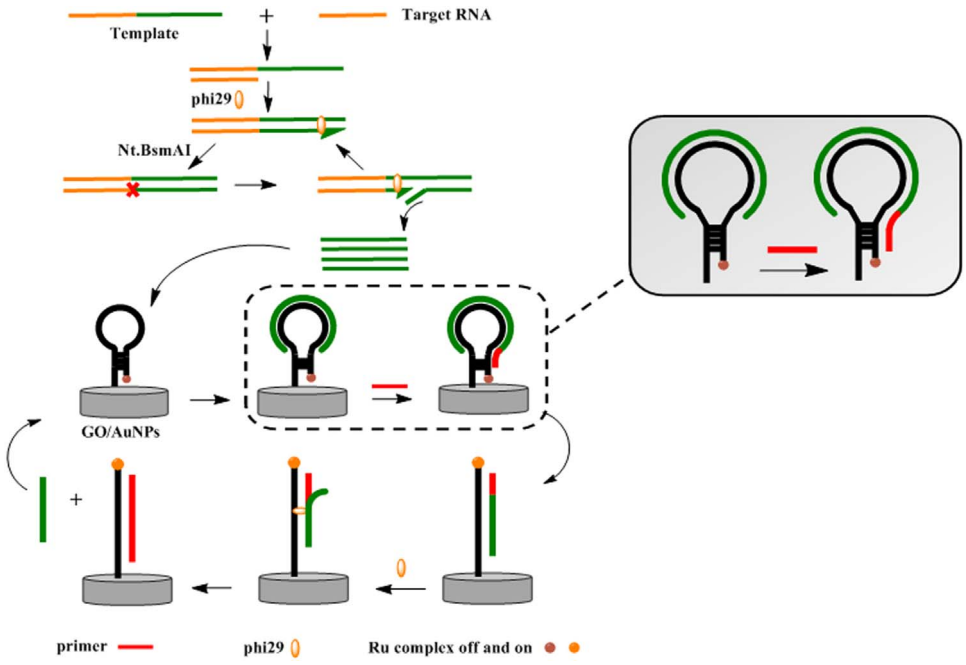

Scheme 1. Schematic illustration of the ECL biosensor fabrication process.

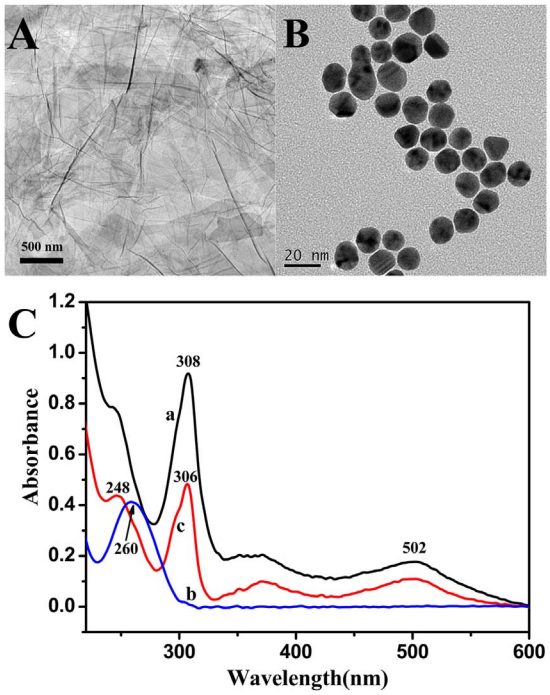

Fig. 1. TEM images of GO (A) and AuNPs (B). (C) UV–vis absorption section of (a) Ru complex; (b) hairpin probe; (c) Ru complex modified hairpin probe in 0.1 M PBS (pH, 7.4).

consistenting with the remarkable peaks of hairpin probe at 260 nm and Ru complex at 308 nm, respectively, indicating that Ru complex modified hairpin probe successfully.

Besides, the characterization of hp-DNA/AuNPs composites, the TEM of GO-AuNPs, the CD spectrum of duplex and hp-DNA and more details were provided in Supplementary material.

3.3. Characterization of the biosensor

The modification process of the biosensor was characterized by EIS in 5 mM $[Fe(CN)_6]^{3-/4-}$ (1:1) solution containing 0.1 M KCl with the frequency from 10^{-1} to 10^5 Hz. As depicted in Fig. 2A, the resistance of the bare GCE was about 360 Ω (curve a). After immobilization of GO on the electrode surface, the resistance obviously increased to 1280 Ω (curve b), which could be ascribed to the electrical insulating properties and negatively charged of GO. Then, AuNPs were dropped on the GO modified GCE, and the resistance markedly decreased (curve c), which depended on the excellent electronic conductivity of AuNPs and the increased electrode surface. After hp-DNA was immobilized on the electrode surface, a clearly increase of resistance was observed (curve d) due to the electrostatic repulsion between the negatively charged phosphoric acid backbone of hp-DNA and $[Fe(CN)_6]^{3-/4-}$. Subsequently, a largely increased resistance was observed (curve e) after hp-DNA was hybridized with the amplification products and primers. It can be attributed to the fact that the stem of the hairpin probe is opened in the presence of the amplification products and primers and then forms a duplex structure which contains more negative phosphate groups and hinders the electron transfer further. Similarly, after the second isothermal strand-displacement polymerase reaction (curve f), resistance increased evidently. It can be attributed to the fact that the ISDPR produced a large amount of duplex structure. These results could confirm the successful fabrication of the biosensor.

3.4. Detection feasibility assay

The detection feasibility assay was testified by comparing the ECL response of electrodes with different modification process in 0.1 M PBS containing 0.1 M TPrA. As seen in Fig. 2B, AuNPs/GO/GCE only presented a weak ECL response (curve a). After immobilization of hp-DNA, the ECL signal increased slightly (curve b), which can be attributed to immobilized Ru complex at the end of hp-DNA. Though the ECL signal was quenched by GO, it still remains weak ECL phenomenon. The increased signal also indicated that the Ru complex has been successfully immobilized to the electrode surface. After hp-DNA was hybridized with the amplification products and primers (curve c), the ECL signal increased significantly, which was ascribed to the formation of linear DNA to keeping the Ru complex away from the electrode surface. Here, it is further demonstrated that the distance between Ru complex and GO affects ECL quenching. A sharper increase in ECL signal was obtained after the second isothermal strand-displacement polymerase reaction (curve d). Obviously, the increased signal was caused by strand displacement and target recycling, which made Ru complex move away from the electrode continuously. Owing to the two-stage isothermal strand-displacement polymerase reaction, a small amount of microRNA can cause a highly ECL response. While the signal is also very stable as shown in the Fig. 2B. According to the above results, we can conclude that this biosensor could be applied for ultrasensitive detection of microRNA.

In addition, the signal amplification effect of ISDPR wsd also proved by comparing the ECL signal with and without ISDPR amplification, and the results were illustrated in Supplementary material (Fig. S2).

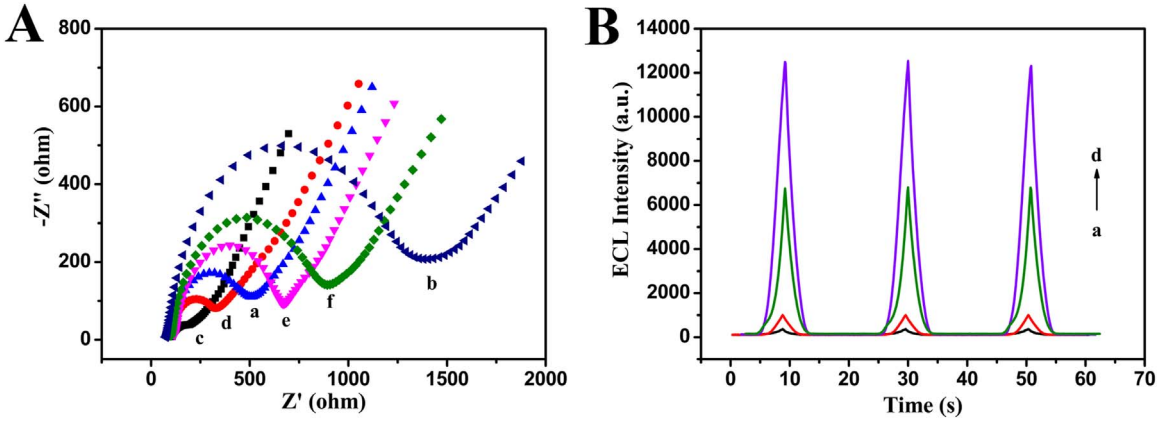

Fig. 2. (A) EIS of GCE (a); GO/GCE (b); AuNPs/GO/GCE (c); hp-DNA/AuNPs/GO/GCE (d); Amplification dsDNA/AuNPs/GO/GCE (e); After the second isothermal strand-displacement polymerase reaction (f) in 5 mM $[Fe(CN)_6]^{3-/4-}$ (1:1) solution containing 0.1 M KCl. (B) ECL intensity of AuNPs/GO/GCE (a), hp-DNA/AuNPs/GO/GCE (b), dsDNA/AuNPs/GO/GCE (c), After the second isothermal strand-displacement polymerase reaction (d).

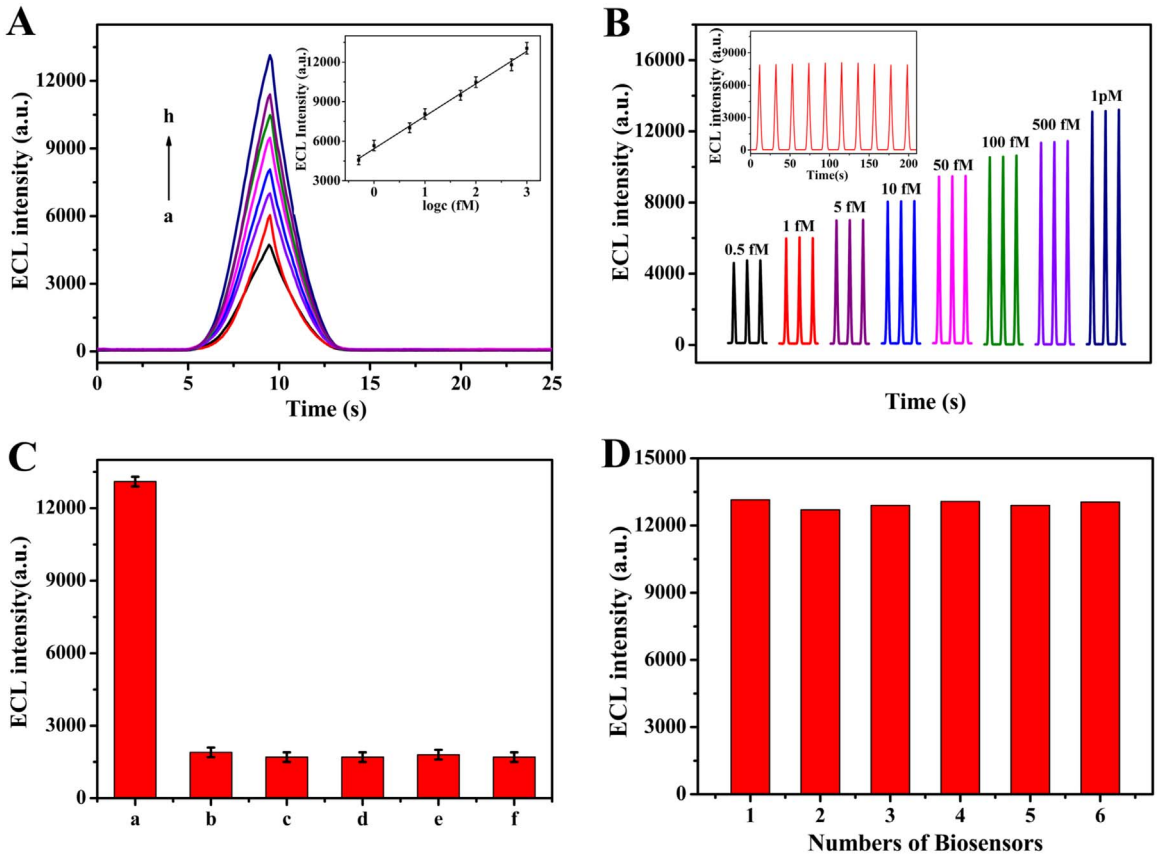

Fig. 3. (A) ECL response for different concentrations of microRNA-319a. a–h, 0.5, 1, 5, 10, 50, 100, 500, 1000 fM. Inset: calibration curve. (B) ECL stability of the biosensor to different concentrations of microRNA. Inset: ECL responses of the biosensor in 10 cycles (the concentration of miRNA is 10 fM). (C) Specificity of the biosensor: (a), microRNA-319a, (b) microRNA-395f, (c), microRNA-393a, (d) microRNA-319b, (e) microRNA-393b, (f), blank (The concentration of microRNA is 1000 fM). (D) The reproducibility of six biosensors fabricated dependently.

3.5. Optimum of experiment conditions

To improve the detection sensitivity and efficiency of the biosensor, several parameters were optimized, such as template DNA concentration, polymerase reaction time, hairpin probe concentration, and primer concentration (The detailed data was listed in Supplementary material, Fig. S1). The optimizal condition was as follows, template DNA concentration, 100 nM; strand displacement reaction time, 2.5 h; hairpin probe concentration, 1 μM; primer concentration, 0.5 μM.

3.6. Detection performances

Under the optimal experiment conditions, the ECL response of the biosensor was analyzed with different concentrations of microRNA-319a. As depicted in Fig. 3A, the ECL response increased with increasing microRNA-319a concentration from 0.5 to 1000 fM. A linear relationship can be gotten between ECL response and the logarithm value of microRNA-319a concentration. The linear regression equation was $I = 2465.17 \log c$ (fM) + 5431.28 with the correlation coefficient of 0.9949. The detection limit was calculated to be 0.14 fM (S/N = 3). Compared with the detection limit and the linear range of previous work, this biosensor performed excellent microRNA detection performance. The comparison results were listed in Table 1.

The stability is a key parameter for the ECL biosensor, and it was investigated by detecting the ECL response of different concentrations of microRNA-319a. As show in Fig. 3B, the biosensors were very stable under three cycles at different concentrations, and there was no significant change of ECL response observed even in ten cycles with the microRNA-319a concentration of 10 fM (In the inset of Fig. 3B,). These results demonstrated that the stability of the biosensor was excellent.

Table 1
A comparison of the developed method with other reported methods.

Methods	Linear range (fM)	LOD (fM)	Refs.
Electrochemistry	100–500,000	84.3	(Rafieepour et al., 2016)
Electrochemistry	1–100,000	0.36	(Li et al., 2016)
Electrochemistry	10–10,000,000	9	(Ma et al., 2016)
Fluorescence	10–10,000	7.3	(Lv et al., 2016)
Fluorescence	1–50,000	0.27	(Yin et al., 2017)
Fluorescence	1000–1,000,000	100	(Chi et al., 2017)
Photoelectrochemistry	1–500	0.56	(Li et al., 2015)
Photoelectrochemistry	350–5,000,000	153	(Tu et al., 2016)
Photoelectrochemistry	5–3000	2.26	(Yin et al., 2016)
ECL	0.1–1000	0.022	(Chen et al., 2016)
ECL	0.1–10,000	0.03	(Yu et al., 2016)
ECL	100–10,000,000	100	(Zhang et al., 2016)
ECL	0.5–1000	0.14	This work

Detection specificity is a critical parameter for an analytical method. The detection specificity of the this method was assessed by hybridizing the template DNA with five kinds of different microRNA sequences and blank (without any microRNA) at the same concentration (1 pM), including complementary microRNA (microRNA-319a), microRNA-395f, microRNA-393a, microRNA-319b and microRNA-393b. As presented in Fig. 3C, the ECL intensity for microRNA-319a was significantly higher than that of other four microRNAs, indicating that the fabricated biosensor can excellent discriminate target microRNA-319a and four other microRNAs. It can be ascribed to the fact that the other microRNAs can not efficiently hybridize with template DNA, which resulted in the low amount of trigger DNA. The results indicated that the developed method had good detection specificity.

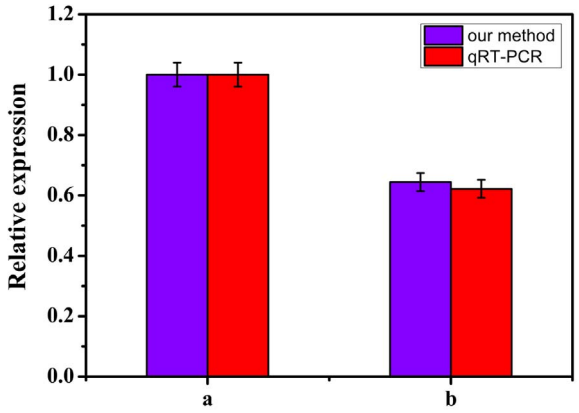

Fig. 4. The relative expression level of microRNA-319a in EMS treated seedlings (a) and normal seedlings (b).

Reproducibility is another critical parameter to estimate a method. For testifying the reproducibility of the biosensor, six biosensors were fabricated independently with microRNA-319a concentration of 1 pM (Fig. 3D). The relative standard deviation (RSD) for the six biosensors was 1.3%, indicating that this biosensor possessed satisfactory detection reproducibility.

Shelf life of the biosensor was also investigated and the results were listed in Supplementary material.

3.7. Sample assay

In order to assess the applicability of the ECL biosensor in real samples, the effect of EMS on the expression levels variation of microRNA-319a in the leaves of rice seedlings was surveyed. For performing it, the rice seeds was immersed in aqueous solutions of ethyl methanesulfonate for six hours. Afterwards, the total RNA was extracted from the rice leaves and the ECL response of microRNA-319a in total RNA was tested. As shown in Fig. 4, the ECL response of microRNA-319a increased with the addition of ethyl methanesulfonate, indicating that ethyl methanesulfonate influence the expression of miRNA and therefore might have an impact on the growth and development of plants. For assessing the accuracy of this method, the expression level of microRNA-319a was also evaluated by qRT-PCR. As illustrated in Fig. 4, the results were consistent with them observed by the method we developed, indicating the veracity of our method.

4. Conclusions

In summary, a sensitive electrochemiluminescence method was developed for microRNA-319a detection based on two-stage isothermal strand-displacement polymerase reaction. After the two-stage amplification, a small amount of target microRNA-319a can produce a great number of trigger DNA to emit the ECL signal. Based on the specific hybridization of template DNA and microRNA-319a, the biosensor exhibited excellent selectivity for different microRNA sequences. The fabricated biosensor also presented a good detection sensitivity with a low detection limit of 0.14 fM and a wide linear range from 0.5 to 1000 fM. Moreover, the application in rice seedlings indicated that the biosensor could display good performance in real sample. Thus the developed electrochemiluminescence method might be a prospective detection tool for microRNA-319a detection in biology research.

Acknowledgements

This work was supported by the Natural Science Foundation of Shandong Province of China (No. ZR2014BQ029), the National Natural Science Foundation of China (No. 21375079), Project of the Distinguished Young Scholar of Shandong Agricultural University, Founds of Shandong “Double Tops” Program (SYL2017XTTD15).

Appendix A. Supplementary material

Supplementary data associated with this article can be found in the online version at http://dx.doi.org/10.1016/j.bios.2018.02.015.

References

Arata, H., Komatsu, H., Han, A., Hosokawa, K., Maeda, M., 2012. Analyst 137, 3234–3237.
Chen, A., Ma, S., Zhuo, Y., Chai, Y., Yuan, R., 2016. Anal. Chem. 88, 3203.
Chi, B.Z., Liang, R.P., Qiu, W.B., Yuan, Y.H., Qiu, J.D., 2017. Biosens. Bioelectron. 87, 216.
Cui, L., Lu, M., Yang, X.Y., Tang, B., Zhang, C.Y., 2017. Analyst 142, 1562–1568.
Feng, X., Gan, N., Zhang, H., Li, T., Cao, Y., Hu, F., Jiang, Q., 2016. Biosens. Bioelectron. 75, 308–314.
Goo, N.I., Kim, D.E., 2016. Biochip J. l1–l10.
Huang, X., Huang, X., Zhang, A., Zhuo, B., Lu, F., Chen, Y., Gao, W., 2015. Biosens. Bioelectron. 70, 441–446.
Kim, D.M., Seo, J., Jun, B.H., Dong, H.K., Jeong, W., Hwang, S.H., Kim, D.E., 2017. Sens. Actuators B Chem. 251, 894–901.
Li, B., Li, X., Wang, M., Yang, Z., Yin, H., Ai, S., 2015. J. Solid State Electrochem. 19, 1301–1309.
Li, B., Liu, F., Peng, Y., Zhou, Y., Fan, W., Yin, H., Ai, S., Zhang, X., 2016. Biosens. Bioelectron. 79, 307–312.
Liu, H., Weng, L., Yang, C., 2017a. Microchim. Acta 184, 1267–1283.
Liu, J., Lu, Y., 2006. Nat. Protoc. 1, 246–252.
Liu, Q., Ma, C., Liu, X.P., Wei, Y.P., Mao, C.J., Zhu, J.J., 2017b. Biosens. Bioelectron. 92, 273–279.
Liu, W., Zhu, M., Liu, H., Wei, J., Zhou, X., Xing, D., 2016. Biosens. Bioelectron. 81, 309–316.
Lv, W., Zhao, J., Situ, B., Li, B., Ma, W., Liu, J., Wu, Z., Wang, W., Yan, X., Zheng, L., 2016. Biosens. Bioelectron. 83, 250–255.
Ma, W., Bo, S., Lv, W., Li, B., Yin, X., Vadgama, P., Zheng, L., Wang, W., 2016. Biosens. Bioelectron. 80, 344–351.
Qian, Y., Tang, D., Du, L., Zhang, Y., Zhang, L., Gao, F., 2015. Biosens. Bioelectron. 64, 177–181.
Rafieepour, H.A., Behpour, M., Keshavarz, M., 2016. Biosens. Bioelectron. 77, 202–207.
Rigoutsos, I., Furnari, F., 2010. Nature 465, 1016–1017.
Schwarzkopf, M., Pierce, N.A., 2016. Nucleic Acids Res. 44 (e129-e129).
Tu, W., Cao, H., Long, Z., Bao, J., Liu, X., Dai, Z., 2016. Anal. Chem. 88.
Wang, M., Yin, H., Shen, N., Xu, Z., Sun, B., Ai, S., 2014. Biosens. Bioelectron. 53, 232–237.
Wang, T., Zhang, Z., Li, Y., Xie, G., 2015. Sens. Actuators B Chem. 221, 148–154.
Wang, X., Liu, W., Yin, B., Sang, Y., Liu, Z., Dai, Y., Duan, X., Zhang, G., Ding, S., Tao, Z., 2017. Microchim. Acta 184, 1603–1610.
Winter, J., Jung, S., Keller, S., Gregory, R.I., Diederichs, S., 2009. Nat. Cell Biol. 11, 228.
Xie, P., Zhu, L., Shao, X., Huang, K., Tian, J., Xu, W., 2016. Sci. Rep. 6, 29524.
Yin, H., Zhou, Y., Li, B., Li, X., Yang, Z., Ai, S., Zhang, X., 2016. Sens. Actuators B Chem. 222, 1119–1126.
Yin, H.S., Li, B.C., Zhou, Y.L., Wang, H.Y., Wang, M.H., Ai, S.Y., 2017. Biosens. Bioelectron. 96, 106–112.
Yu, Y.Q., Wang, J.P., Zhao, M., Hong, L.R., Chai, Y.Q., Yuan, R., Zhuo, Y., 2016. Biosens. Bioelectron. 77, 442–450.
Zhang, M., Li, R., Ling, L., 2017. Anal. Bioanal. Chem. 409, 4079–4085.
Zhang, T., Zhao, H., Fan, G., Li, Y., Li, L., Quan, X., 2016. Electrochim. Acta 190, 1150–1158.
Zhou, X., Zhu, D., Liao, Y., Liu, W., Liu, H., Ma, Z., Xing, D., 2014. Nat. Protoc. 9, 1146–1159.